



# HHS Public Access

Author manuscript

*Nat Cell Biol.* Author manuscript; available in PMC 2014 July 01.

Published in final edited form as:

*Nat Cell Biol.* 2014 January ; 16(1): 99–107. doi:10.1038/ncb2889.

## Stem cell quiescence acts as a tumor suppressor in squamous tumors

AC White<sup>1,2</sup>, JK Khoo<sup>1,2</sup>, CY Dang<sup>1,2</sup>, J Hu<sup>1,2</sup>, KV Tran<sup>1,2</sup>, A Liu<sup>1,2</sup>, S Gomez<sup>1,2</sup>, Z Zhang<sup>3</sup>, R YI<sup>3</sup>, P Scumpia, M Grigorian<sup>1,2</sup>, and WE Lowry<sup>1,2,4,5</sup>

<sup>1</sup>Department of Molecular Cell and Developmental Biology, UCLA

<sup>2</sup>Eli and Edythe Broad Center for Regenerative Medicine, UCLA

<sup>3</sup>Department of Molecular, Cellular, and Developmental Biology, University of Colorado, Boulder, CO 80309 USA

<sup>4</sup>Jonsson Cancer Research Center, UCLA

<sup>5</sup>Molecular Biology Institute, UCLA

### Abstract

In some organs, adult stem cells are uniquely poised to serve as cancer cells of origin. It is unclear, however, whether tumorigenesis is influenced by the activation state of the adult stem cell. Hair follicle stem cells (HFSCs) act as cancer cells of origin for cutaneous squamous cell carcinoma (SCC) and undergo defined cycles of quiescence and activation. The data presented here show that HFSCs are unable to initiate tumors during the quiescent phase of the hair cycle, indicating that the mechanisms that keep HFSCs dormant are dominant to the gain of oncogenes (Ras) or the loss of tumor suppressors (p53). Furthermore, Pten activity is necessary for quiescence based tumor suppression, as its deletion alleviates tumor suppression without affecting proliferation. These data demonstrate that stem cell quiescence is a form of tumor suppression in HFSCs, and that Pten plays a role in maintaining quiescence in the presence of tumorigenic stimuli.

### Introduction

Most mammalian organs contain a resident population of stem cells that serve to replenish tissue in response to injury or for homeostatic turnover. In many cases, stem cells (SCs) have high proliferative capacity, but remain quiescent in comparison to their descendant progenitor cells<sup>5</sup>. In some tissues, such as the epidermis, SCs cycle through activation and quiescence<sup>6</sup>. Recent evidence has shown that for many organs, the resident adult stem cells can also be cancer cells of origin<sup>1-4</sup>, yet it remains unclear how the natural cycling properties of adult stem cells contribute to tumor initiation. Hair follicles are found either in anagen, where the follicle is completely formed and produces a hair shaft, or in telogen, where the follicle is in a quiescent or resting state<sup>7</sup>. In fact, HFSCs rarely divide during

Users may view, print, copy, download and text and data- mine the content in such documents, for the purposes of academic research, subject always to the full Conditions of use: [http://www.nature.com/authors/editorial\\_policies/license.html#terms](http://www.nature.com/authors/editorial_policies/license.html#terms)

To whom correspondence should be addressed: William E Lowry UCLA, Department of Molecular Cell and Developmental Biology 621 Charles Young Drive South Los Angeles, CA 90095 310-794-5175 [blowry@ucla.edu](mailto:blowry@ucla.edu).

either telogen or full anagen, but instead undergo a burst of proliferation only at the start of anagen<sup>8</sup>.

The standard means used to chemically induce epidermal tumors and squamous cell carcinoma (SCC) in mice is the two-step DMBA/TPA carcinogenesis assay<sup>9,10</sup>. DMBA/TPA reliably produces benign hyperplasias called papillomas, and in some cases, these papillomas progress to bona fide SCC. In 1956, it was argued that carcinogens must be applied during telogen to successfully induce tumorigenesis, while subsequent efforts instead suggested that anagen was required for tumor initiation<sup>11,12</sup>. In 1993, Miller et al. showed that the two-step carcinogenesis protocol needed to be initiated during a telogen to anagen transition for tumorigenesis to occur<sup>13,14</sup>. This led to speculation that if the hair cycle controls tumorigenic sensitivity, a likely culprit could be stem cells and the regulation of their activation. Induction of anagen exacerbates progression of Basal Cell Carcinoma (BCC), but is not required for initiation of phenotype<sup>15</sup>, demonstrating that quiescence in telogen is not a barrier to tumorigenesis for BCC<sup>15,16</sup>.

It has been shown that HFSCs are sufficient to act as SCC cancer cells of origin using inducible, cell type specific, genetically defined mouse models<sup>1,2,17</sup>. However, these studies did not address a role for the hair cycle or stem cell activation during tumorigenesis. Here we demonstrate that HFSCs cannot initiate *Kras*<sup>G12D</sup> or *Kras*<sup>G12D</sup>/p53<sup>ff</sup> mediated tumorigenesis in quiescent HFSCs during telogen. Instead, tumorigenesis only begins when HFSCs are released from quiescence during a telogen to anagen transition.

## Results

### Identification of stem cell quiescence mediated tumor suppression

To determine which cells of the hair follicle are capable of initiating tumors that lead to cutaneous cancers, an inducible conditional strategy was employed to deliver tumorigenic stimuli to SCs or transit-amplifying (TA) cells within the hair follicle<sup>1,2</sup>. These experiments showed that HFSCs were cells of origin for SCC, while their TA progeny were unable to generate benign tumors<sup>1,2</sup>, but neither of these studies addressed whether stem cell activation plays a role in tumorigenesis.

In fact, there is a striking effect of the hair cycle on tumor initiation in this model. Treating *K15-CrePR;Kras*<sup>G12D</sup> animals with the progesterone receptor antagonist mifepristone initiates a recombination that removes a stop codon upstream of the constitutively active *Kras*<sup>G12D</sup> knock-in allele and induces expression in the stem cell compartment (the bulge). HFSC driven tumorigenesis was morphologically evident as a hyperplastic bulge at the telogen to anagen transition when Ras was activated either immediately prior to the transition in telogen (Fig 1A)<sup>2</sup> or during the transition (Supplementary Fig 1A). Hyperplasia of the follicle was also evident at two weeks following the telogen to anagen transition, when mifepristone was administered one week prior to the telogen to anagen transition (n = 3 mice) (Fig 1B). In contrast, when *Kras*<sup>G12D</sup> was expressed during telogen for up to ten weeks without a telogen to anagen transition, no morphological evidence of bulge hyperplasia (n = 5 mice) (Fig. 1C, D) or induction of proliferation (Supplementary Fig 1B) was evident, consistent with a lack of sensitivity to oncogenic Ras during HFSC quiescence.

Taken together, these data suggest that *Kras*<sup>G12D</sup>-induced hyperplasias can arise immediately from HFSCs when active during the telogen to anagen transition, but are unable to form hyperplasias when quiescent, even up to ten weeks post induction.

To address whether the response of HFSCs to *Kras*<sup>G12D</sup> is specific to particular portions of the hair cycle, animals were treated with mifepristone during full anagen, at which time HFSCs have returned to a quiescent state. Two weeks following mifepristone administration, anagen hair follicles returned to telogen without exhibiting hyperplasia (n=5 mice) (Supplementary Fig 1C). HFSCs from both the control and *Kras*<sup>G12D</sup> expressing anagen follicles did not exhibit proliferation during this period, as shown by lack of Ki67 staining (Supplementary Fig 1D). These data demonstrate that induction of *Kras*<sup>G12D</sup> expression during anagen is not sufficient to initiate hyperplasia. Together, these data suggested that tumor initiation from HFSCs requires a telogen to anagen transition.

To rule out the possibility that differential recombination efficiency could lead to the disparity in phenotype, we used a YFP lineage tracing allele to quantify recombination at various time points in the protocol. During telogen, the recombination efficiency was 21% +/- 4% after 4 days (n = 25 follicles), and the number of recombined cells did not significantly change upon subsequent quantifications at 14, 21, and 28 days (30% ± 6%, 28% ± 2%, and 22% ± 3%, respectively). Similarly, mice pulsed with mifepristone for four days during anagen showed 21% recombination. This provides further evidence that a significant portion of bulge cells received the oncogenic stimulus in telogen, that these cells remained quiescent and that recombination frequency was affected by the hair cycle.

### Correlation of the hair cycle and SCC in human skin

To determine whether the hair cycle plays a role in initiation of human SCC, we assessed whether any correlation exists between the hair cycle and SCCs in human skin. Both SCC *in situ* (SCCIS) and invasive SCC were quantified by morphological analysis across hundreds of follicles. The closest terminal hair to the tumor was examined for stage of hair cycle. Anagen was associated with 25/25 invasive SCC cases examined and in 38/41 SCC *in situ* cases examined (Fig 1G). Despite the fact that ~90% of hairs are typically in anagen in human skin, these numbers suggest a strong correlation between SCC and the active phase of the hair cycle.

### Pten activity maintains SC quiescence in response to Ras activation

Since the PI3K pathway is activated downstream of Ras, we investigated whether negative regulators of the PI3K pathway were expressed during telogen, in the presence or absence of oncogene activation. Pten, a phosphatase that directly inactivates Akt, was identified as a likely candidate. Staining with a Pten antibody confirmed its presence in control telogen HFSCs (Supplementary Fig 1E). To determine whether Pten prevents initiation of *Kras*<sup>G12D</sup> induced tumorigenesis from telogen HFSCs, we bred animals harboring a floxed version of the *Pten* allele to the *K15-CrePR;Kras*<sup>G12D</sup> line<sup>18</sup> and treated with mifepristone during telogen (at 7-8 weeks of age). In contrast to *K15-CrePR;Kras*<sup>G12D</sup> bulges, which appeared similar to controls, *K15-CrePR;Kras*<sup>G12D</sup>;*Pten*<sup>ff</sup> hair follicles demonstrated hyperplastic expansion during telogen (Fig 1E and Supplementary Fig 1E). Hyperplastic phenotypes

were found in  $26.9 \pm 4.4\%$  of all examined hair follicles in *K15-CrePR;Kras<sup>G12D</sup>;Pten<sup>ff</sup>* skin (n = 3 mice, n = 1,361 follicles quantified). Additionally, immunostaining for Pten showed that these hyperplastic structures appeared to have reduced or absent Pten expression (Supplementary Fig 1E). To address whether loss of a single allele of *Pten* would suffice to promote proliferation in the context of *Kras<sup>G12D</sup>*, *K15-CrePR;Kras<sup>G12D</sup>;Pten<sup>wf</sup>* mice were generated. Four weeks post mifepristone treatment, *K15-CrePR;Kras<sup>G12D</sup>;Pten<sup>wf</sup>* skin did not exhibit bulge hyperplasias (n = 3 mice) (Supplementary Fig 1F).

### Pten does not control hair cycle initiation or proliferation

Two hypotheses could explain why *K15-CrePR;Kras<sup>G12D</sup>;Pten<sup>ff</sup>* bulges produced hyperplasias during telogen. *Pten* deletion could induce a hair cycle *de novo* and thus allow for a response to *Kras<sup>G12D</sup>* activity or it could act to block to *Kras<sup>G12D</sup>* mediated downstream pathways during telogen. To distinguish between these two possibilities, *K15-CrePR;Pten<sup>ff</sup>* mice were generated to ablate *Pten* during telogen without inducing *Kras<sup>G12D</sup>*. Four weeks after induction of *Pten* deletion at 7-8 weeks of age, telogen *K15-CrePR;Pten<sup>ff</sup>* follicles did neither spontaneously initiate a hair cycle (Fig 1F) nor increase in proliferation (Supplementary Fig 1G). Though Pten appeared to be upregulated at the telogen to anagen transition in controls (Supplementary Fig 1H), Pten staining appeared absent during a naturally occurring transition in *K15-CrePR;Pten<sup>ff</sup>* skin (Supplementary Fig 1I), demonstrating effective *Pten* deletion. Taken together, these data suggest that Pten does not simply prevent entry into the hair cycle but instead acts to block a tumorigenic response to oncogenic Ras in quiescent HFSCs.

### Telogen bulge hyperplasias do not arise from Lgr5<sup>+</sup> or Lgr6<sup>+</sup> cells

To refine the cells of origin for hyperplasias arising from telogen HFSCs, we employed alternative Cre drivers to express *Kras<sup>G12D</sup>* and thereby conditionally delete *Pten*. Whereas the *K15-CrePR* allele targets the entire bulge and hair germ, expression of the *Lgr5-CreER* allele is restricted to the hair germ and the lower region of the telogen bulge<sup>19</sup>. *Lgr5-CreER;Kras<sup>G12D</sup>;Pten<sup>ff</sup>* animals were bred to determine if the hair germ and lower bulge were sufficient to promote hyperplasia. Four weeks post tamoxifen treatment, telogen hair follicle bulges demonstrated no morphological change, indicating that the *Lgr5* expressing population were not the cells of origin in this context (n = 3 mice) (Fig 2A).

The *Lgr6-CreER* allele, which targets cells immediately above the bulge, as well as isolated cells of the interfollicular epidermis, was employed to further define the cells of hyperplasia origin<sup>20</sup>. Rare hyperplasias were found arising from *Lgr6-CreER;Kras<sup>G12D</sup>;Pten<sup>ff</sup>* hair follicles, but these were morphologically distinct from those found in *K15-CrePR;Kras<sup>G12D</sup>;Pten<sup>ff</sup>* telogen bulges (n = 3 mice). The phenotypes included hyperplasia of the sebaceous gland, infundibulum and interfollicular epidermis (Fig 2B). In all cases, telogen bulges in *Lgr6-CreER;Kras<sup>G12D</sup>;Pten<sup>ff</sup>* mice remained intact. Furthermore, the hyperplasias formed by the *Lgr6<sup>+</sup>* cells outside the telogen bulge were morphologically distinct. These data indicate that the cells of origin for the hyperplasias found in *K15-CrePR;Kras<sup>G12D</sup>;Pten<sup>ff</sup>* telogen HFSCs reside in the *Lgr5*-upper bulge, below the *Lgr6<sup>+</sup>* population.

## Signaling pathways and transcription factors differentially regulated by loss of *Pten* and stem cell quiescence based tumor suppression

*Pten* acts as a negative regulator of Akt activation downstream of Ras. p-Akt, the activated form of Akt, is only found rarely in cells of control telogen bulges (Fig 3A)<sup>21</sup>. Similar to controls, *K15-CrePR;Kras<sup>G12D</sup>* telogen HFSCs did not show staining throughout this compartment (Fig. 3A and Supplementary Fig 2A) and *Pten*-only deletion was not sufficient to activate Akt (Supplementary Fig 2A). Consistent with the mechanism of *Pten* activity, *Pten* deletion in the presence of *Kras<sup>G12D</sup>* expression resulted in high p-Akt staining in hyperplastic bulges (Fig 3A). Non-phosphorylated Akt, was found in control telogen HFSCs, thus the change in activity was attributable to phosphorylation rather than a change in expression level (Supplementary Fig 1J). These observations suggest that quiescent SCs are refractory to the activation of Akt by *Kras<sup>G12D</sup>* through *Pten* and that Akt is a mediator of hyperplastic expansion. In addition to repression of Akt signaling, *Pten* has also been shown to repress the transcription factor activities of Creb and cJun<sup>22-24</sup>. Nuclear localization of p-Creb and p-cJun were found at high levels in hyperplastic bulges (Fig 3B, C), but not in normal skin (Fig 3B, C, and Supplementary Fig 2B, C). This is also interesting in light of data showing that Creb or Jun inhibition abrogates papilloma formation<sup>25,26</sup>. To characterize the hyperplastic bulges in *K15-CrePR;Kras<sup>G12D</sup>;Pten<sup>ff</sup>* skin, a number of hair follicle markers were assessed. Krt14, a marker of basal cells in stratified epithelia, was found throughout hyperplasias exhibiting basal epithelial morphology and in the outer layers of cyst structures (Supplementary Fig 2D). Krt6, a marker of hyperplastic epidermis, was also found throughout bulge hyperplasias (Supplementary Fig 2E). Expression of Sox9, a HFSC marker, was found throughout the phenotypes that developed (Supplementary Fig 2F), most likely due to expansion of the bulge population.

## Understanding mechanisms of tumor initiation through gene expression profiling

To identify the molecular basis for tumor suppression through stem cell quiescence, cells from induced *K15-CrePR;LSLYFP*, *K15-CrePR;Kras<sup>G12D</sup>;LSLYFP* and *K15-CrePR;Kras<sup>G12D</sup>;Pten<sup>ff</sup>;LSLYFP* skin were FACS isolated by YFP expression. Differential transcription profiles were generated by microarray comparing YFP<sup>+</sup> cells from *K15-CrePR;LSLYFP* to *K15-CrePR;Kras<sup>G12D</sup>;Pten<sup>ff</sup>;LSLYFP* and *K15-CrePR;Kras<sup>G12D</sup>;LSLYFP* telogen bulges, four weeks following mifepristone treatment. A striking pattern emerged whereby some of the factors thought to regulate the telogen to anagen transition were differentially regulated in *K15-CrePR;Kras<sup>G12D</sup>;Pten<sup>ff</sup>* mice as compared to controls (Fig 4A)<sup>27</sup> including: Tgfβ(induced), Egf (induced), Bmp and Fgf (suppressed). In general, these data suggested that *Pten* deletion during telogen led to decreased expression of genes previously shown to promote the quiescent telogen state, while most of the genes thought to play a role in driving anagen were not induced. This indicates that Ras activation coupled with *Pten* deletion gives rise to HFSCs that are deinhibited by telogen and sensitive to tumor initiation.

Since micro-RNAs (miRNAs) can regulate large sets of genes, miRNA profiling was employed to understand how some of the expression changes that underlie quiescence based tumor suppression in HFSCs originated. YFP<sup>+</sup> cells from *K15-CrePR;LSLYFP* telogen bulges and *K15-CrePR;Kras<sup>G12D</sup>;Pten<sup>ff</sup>;LSLYFP* telogen bulges were collected by FACS on

the basis of YFP expression and profiled. 30 miRNAs were found to be induced at least 1.5 fold in *K15-CrePR;Kras<sup>G12D</sup>;Pten<sup>ff</sup>* bulges (Supplementary Fig 3A), and some of these changes were confirmed by RT-PCR on an independent sample (Fig 4B). The targets of seven upregulated miRNA families were found enriched amongst downregulated mRNAs detected by microarray profiling (Fig 4B) suggesting that upregulation of these miRNAs played a functional role in the downregulation of a number of mRNAs (Fig 4B). Interestingly, miR-21, the miRNA shown to have the highest number of relative differentially regulated targets, has been shown in numerous contexts to be induced by Tgf $\beta$  and Bmp activation<sup>28-32</sup>, and ablation of miR-21 abrogated squamous tumorigenesis in a DMBA/TPA protocol<sup>33-36</sup>.

The signaling pathways suggested by the gene expression data as differentially activated were also assessed at the protein level. The Tgf $\beta$  pathway is activated during the telogen to anagen transition<sup>37</sup>, and was induced, as determined by phosphorylation of the effector protein Smad2, in *K15-CrePR;Kras<sup>G12D</sup>;Pten<sup>ff</sup>* hyperplastic bulges (Fig 4D) but absent in control, *K15-CrePR;Kras<sup>G12D</sup>* and *K15-CrePR;Pten<sup>ff</sup>* bulges (Supplementary Fig 4A). Next, *K15-CrePR;Kras<sup>G12D</sup>;Pten<sup>ff</sup>* hyperplasias stained strongly for active Egf receptor signaling (Fig 4E), but was weak or absent in control, *K15-CrePR;Kras<sup>G12D</sup>* and *K15-CrePR;Pten<sup>ff</sup>* bulges (Supplementary Fig 4B)<sup>38</sup>. Wnt signaling, also thought to promote HFSC activation and the telogen to anagen transition<sup>39</sup>, was not induced in hyperplasia as assayed by nuclear localization of  $\beta$ -catenin and expression of known transcriptional targets of the Wnt pathway (Supplementary Fig 4E). These data demonstrate that some activators of the hair cycle are present during *K15-CrePR;Kras<sup>G12D</sup>;Pten<sup>ff</sup>* hyperplasia formation in telogen HFSCs but Wnt was not.

*Fgf18* plays a critical role in telogen, as ablation of *Fgf18* dramatically shortens this quiescent phase<sup>40</sup>. Here, we found that staining with an Fgf18 antibody showed significantly reduced expression in *K15-CrePR;Kras<sup>G12D</sup>;Pten<sup>ff</sup>* telogen bulges (Fig 4F), but not in *K15-CrePR;Kras<sup>G12D</sup>* and *K15-CrePR;Pten<sup>ff</sup>* telogen bulges (Supplementary Fig 4C). Bmp signaling is also thought to maintain telogen and activity of this pathway can be measured by phosphorylation of Smad1/5/8<sup>41</sup>. Consistent with this, we observed downregulation of Bmp ligands in *K15-CrePR;Kras<sup>G12D</sup>;Pten<sup>ff</sup>* hyperplasias (Fig 4A). Unexpectedly, nuclear p-Smad1/5/8 stained strongly in proliferating *K15-CrePR;Kras<sup>G12D</sup>;Pten<sup>ff</sup>* bulges and in hyperplastic structures (Fig 4G), but not in *K15-CrePR;Kras<sup>G12D</sup>* and *K15-CrePR;Pten<sup>ff</sup>* HFSCs (Supplementary Fig 4D).

To summarize, *K15-CrePR;Kras<sup>G12D</sup>;Pten<sup>ff</sup>* telogen bulges exhibited three features of activated HFSCs, notably high Tgf $\beta$  and Egf activity and low *Fgf18* expression, while failing to exhibit other features, such as induction of Wnt or suppression of Bmp signaling. Thus, *K15-CrePR;Kras<sup>G12D</sup>;Pten<sup>ff</sup>* bulges exist in an atypical state that allows for oncogenic Kras to promote hyperplasia in a normally refractive SC niche via only partially activated HFSCs.

### Quiescent HFSCs are refractory to *Kras<sup>G12D</sup>*; *p53<sup>ff</sup>* cancer initiation

*K15-CrePR;Kras<sup>G12D</sup>;p53<sup>ff</sup>* mice did not initiate SCC while HFSCs were in telogen (Fig 5A, B). Therefore, to determine whether Pten plays a role in stem cell quiescence mediated

prevention of carcinoma initiation we generated *K15-CrePR;Kras<sup>G12D</sup>;p53<sup>ff</sup>;Pten<sup>ff</sup>* animals and examined them up to 4 weeks after mifepristone administration during telogen. In a striking departure from *K15-CrePR;Kras<sup>G12D</sup>;p53<sup>ff</sup>* animals, these animals produced macroscopically identifiable skin phenotypes one to two weeks following induction with mifepristone (n = 4 mice). The skin malignancies that formed showed features of malignant trichoblastoma, malignant tricholemmoma, desmoplastic squamous cell carcinoma and spindle-cell squamous cell carcinoma (Fig 5C, D, E, F). Consistent with these findings, tricholemmomas are characteristic of Cowden's disease, which occurs in human patients with *Pten* mutations<sup>42</sup>.

The signaling pathways previously implicated in the hyperplasias of *K15-CrePR;Kras<sup>G12D</sup>;Pten<sup>ff</sup>* HFSCs were re-examined in the context of *K15CrePR;Kras<sup>G12D</sup>;p53<sup>ff</sup>;Pten<sup>ff</sup>* malignancies. These tumors contained an epithelial component that retained E-cadherin expression, as well as a Vimentin expressing mesenchymal component that was composed of either cancer associated fibroblasts or tumor cells that had undergone an epithelial to mesenchymal transition (Fig 6A), also suggested by some of the cells at the invasive front expressing both Keratin 5 and Vimentin (Supplementary Fig 4F). The E-Cad<sup>+</sup> tumor cells demonstrated high levels of p-Creb, p-Smad2, p-Smad1/5/8 and p-Egfr (Fig 6C, E, F, G, third panel), consistent with the notion that these pathways contribute to progression. In contrast to *K15-CrePR;Kras<sup>G12D</sup>;Pten<sup>ff</sup>* hyperplasias, these malignancies showed low p-Akt and low pcJun staining, suggesting that these pathways might not be critical for tumor progression (Fig 6B, D, third panel).

## Discussion

Using the hair follicle as a model system for tumorigenesis with a stem cell origin, we explored the potential influence of the cycling nature of stem cell activation and quiescence in tumor initiation. The data presented here demonstrate that quiescence can be utilized to suppress tumorigenesis in stem cells harboring cancer-causing mutations. Adult stem cell activation occurs with varying frequencies in several organs, including almost continuously (intestine), cyclically (hair follicle), infrequently (mammary gland) or only in situations of necessary repair (prostate). Thus, the frequency of stem cell activation can have important implications when considering the latency of cancer initiation in humans. In some situations, adult stem cells that harbor the necessary mutations to generate a cancerous lesion could lay dormant for decades until activated, such as in cases of stem cell activation due to organ injury.

Induction of oncogenic *Kras* alone or oncogenic *Kras* combined with *p53* knockout in HFSCs is sufficient to initiate tumorigenesis when the stem cells have been activated, but not when these cells lay at rest in quiescence. *Pten* enables quiescence based tumor suppression, since when deleted, quiescent HFSCs are able to initiate tumorigenesis. During the formation and progression of hyperplasias and malignancies arising from telogen stem cells a number of signaling cascades are active, namely the Tgf $\beta$ , Bmp, and Egf pathways (Fig 6). Furthermore, when *Pten* deletion is combined with *Kras<sup>G12D</sup>* expression and *p53* knockout, normally quiescent HFSCs are capable of initiating SCC. Additionally, a distinct set of miRNA families are differentially regulated during emergence of tumorigenesis in

*K15-CrePR;Kras<sup>G12D</sup>;Pten<sup>ff</sup>* skin, some of which appear to play a significant role in mRNA regulation during phenotype progression. Dissecting the intricate web of signaling, transcription factor activity and suppression of gene expression through miRNAs that control quiescence based tumor suppression in HFSCs represents an important avenue of exploration.

These data also revealed an unusual situation in which simultaneous activation of both the Tgf $\beta$  and Bmp arms of the Tgf signaling cascades were found. This was surprising because these pathways are typically antagonistic to each other, particularly in the epidermis<sup>37,41</sup>. In fact, downregulation of Bmp ligands was observed coincident with Tgf $\beta$  activation (Fig 4A), but this did not lead to decreased Smad1/5/8 activation (Fig 4G). Regardless, these results are evidence that loss of *Pten* combined with Ras activation promotes some aspects of anagen (Tgf $\beta$  signaling) while failing to remove some inhibitory aspects of telogen (Bmp signaling). This is consistent with the fact that a normal anagen follicle does not form in this setting.

The work presented here does not preclude a role for SCC initiation from the interfollicular epidermis (IFE). It is clear from work with human keratinocytes that cutaneous tumorigenesis can be initiated in the absence of hair follicles<sup>43</sup>. It remains controversial as to whether a hierarchy of developmental potential exists in the interfollicular epidermis or whether cells of the IFE cycle through periods of quiescence and activation. Due to these limitations, it is difficult to determine if SC quiescence also plays a role in suppression of tumorigenesis derived from the IFE.

The model presented here demonstrates that *Pten* is a key factor for maintaining HFSC quiescence in the face of oncogene activation, but does not necessarily suggest that *Pten* plays a role in SCC. Instead, *Pten* prevents tumor formation in quiescent HFSCs that normally occurs when Ras is activated. Though *Pten* mutations are not often found in human cutaneous SCC<sup>44-46</sup>, patients with a loss of function mutations in *Pten* (Cowden's Disease), exhibit increased tricholemmoma incidence and a higher risk of SCC<sup>46-48</sup>. These data present a unique conceptual framework for cancer origination, with important implications for a range of tumors arising from various organs, particularly in those where turnover of stem cells is synchronized or that only activate during injury.

## Supplementary Material

Refer to Web version on PubMed Central for supplementary material.

## Acknowledgements

We would like to acknowledge the technical support of Woo Kim; the management of the animal facilities (DLAM); the FACS core (EEBSCRC); the TPCL (Department of Pathology, UCLA); the gene expression core (Department of Pathology, UCLA) and Xavier Gaeta for a critical reading of the manuscript. This work was supported by grants from CIRM (TG2-01169), CRCC, The JCCF, and NIH (UCLA Tumor Biology Program, Ruth L. Kirschstein Institutional National Research Service Award # T32 CA009056, UCLA; and 5R01AR057409-03). WEL holds the Maria Rowena Ross Term Chair in Cell Biology.



## References

1. Lapouge G, et al. Identifying the cellular origin of squamous skin tumors. *Proceedings of the National Academy of Sciences of the United States of America*. 2011; 108:7431–7436. [PubMed: 21502497]
2. White AC, et al. Defining the origins of Ras/p53-mediated squamous cell carcinoma. *Proceedings of the National Academy of Sciences of the United States of America*. 2011; 108:7425–7430. [PubMed: 21502519]
3. Barker N, et al. Crypt stem cells as the cells-of-origin of intestinal cancer. *Nature*. 2009; 457:608–611. [PubMed: 19092804]
4. Visvader JE. Cells of origin in cancer. *Nature*. 2011; 469:314–322. [PubMed: 21248838]
5. Lowry WE, Richter L. Signaling in adult stem cells. *Frontiers in bioscience : a journal and virtual library*. 2007; 12:3911–3927. [PubMed: 17485347]
6. Fuchs E. The tortoise and the hair: slow-cycling cells in the stem cell race. *Cell*. 2009; 137:811–819. [PubMed: 19490891]
7. Paus R, Muller-Rover S, Botchkarev VA. Chronobiology of the hair follicle: hunting the “hair cycle clock”. *J Investig Dermatol Symp Proc*. 1999; 4:338–345.
8. Greco V, et al. A two-step mechanism for stem cell activation during hair regeneration. *Cell Stem Cell*. 2009; 4:155–169. [PubMed: 19200804]
9. Trempus CS, et al. CD34 expression by hair follicle stem cells is required for skin tumor development in mice. *Cancer research*. 2007; 67:4173–4181. [PubMed: 17483328]
10. Finch JS, Albino HE, Bowden GT. Quantitation of early clonal expansion of two mutant 61st codon c-Ha-ras alleles in DMBA/TPA treated mouse skin by nested PCR/RFLP. *Carcinogenesis*. 1996; 17:2551–2557. [PubMed: 9006088]
11. Andreasen E, Borum K. The influence of the mouse hair cycle on 9, 10-dimethyl-1, 2-benzanthracene-induced skin tumors. *Acta Pathol Microbiol Scand Suppl*. 1956; 39:76–77. [PubMed: 13372267]
12. Klinken-Rasmussen L. Effect of croton oil applied to mouse skin originally painted with suboptimal doses of carcinogen during the growth and resting phases of the hair follicles. *Acta Pathol Microbiol Scand Suppl*. 1956; 39:78–79. [PubMed: 13372268]
13. Miller SJ, et al. Mouse skin is particularly susceptible to tumor initiation during early anagen of the hair cycle: possible involvement of hair follicle stem cells. *The Journal of investigative dermatology*. 1993; 101:591–594. [PubMed: 8409528]
14. Lavker RM, et al. Hair follicle stem cells: their location, role in hair cycle, and involvement in skin tumor formation. *The Journal of investigative dermatology*. 1993; 101:16S–26S. [PubMed: 8326150]
15. Grachtchouk M, et al. Basal cell carcinomas in mice arise from hair follicle stem cells and multiple epithelial progenitor populations. *The Journal of clinical investigation*. 2011; 121:1768–1781. [PubMed: 21519145]
16. Mancuso M, et al. Hair cycle-dependent basal cell carcinoma tumorigenesis in Ptc1neo67/+ mice exposed to radiation. *Cancer research*. 2006; 66:6606–6614. [PubMed: 16818633]
17. Li S, et al. A keratin 15 containing stem cell population from the hair follicle contributes to squamous papilloma development in the mouse. *Molecular carcinogenesis*. 2012
18. Groszer M, et al. Negative regulation of neural stem/progenitor cell proliferation by the Pten tumor suppressor gene in vivo. *Science (New York, N.Y.)*. 2001; 294:2186–2189.
19. Jaks V, et al. Lgr5 marks cycling, yet long-lived, hair follicle stem cells. *Nature genetics*. 2008; 40:1291–1299. [PubMed: 18849992]
20. Snippert HJ, et al. Lgr6 marks stem cells in the hair follicle that generate all cell lineages of the skin. *Science (New York, N.Y.)*. 2010; 327:1385–1389.
21. Zhang J, et al. BMP signaling inhibits hair follicle anagen induction by restricting epithelial stem/progenitor cell activation and expansion. *Stem Cells*. 2006
22. Gu T, et al. CREB is a novel nuclear target of PTEN phosphatase. *Cancer research*. 2011; 71:2821–2825. [PubMed: 21385900]

23. Vivanco I, et al. Identification of the JNK signaling pathway as a functional target of the tumor suppressor PTEN. *Cancer cell*. 2007; 11:555–569. [PubMed: 17560336]
24. Tran LM, et al. Determining PTEN functional status by network component deduced transcription factor activities. *PLoS ONE*. 2012; 7:e31053. [PubMed: 22347425]
25. Rozenberg J, et al. Inhibition of CREB function in mouse epidermis reduces papilloma formation. *Mol Cancer Res*. 2009; 7:654–664. [PubMed: 19435810]
26. Ji J, et al. Elevated coding mutation rate during the reprogramming of human somatic cells into induced pluripotent stem cells. *Stem cells*. 2012; 30:435–440. [PubMed: 22162363]
27. Plikus MV. New activators and inhibitors in the hair cycle clock: targeting stem cells' state of competence. *The Journal of investigative dermatology*. 2012; 132:1321–1324. [PubMed: 22499035]
28. Ahmed MI, Mardaryev AN, Lewis CJ, Sharov AA, Botchkareva NV. MicroRNA-21 is an important downstream component of BMP signalling in epidermal keratinocytes. *Journal of cell science*. 2011; 124:3399–3404. [PubMed: 21984808]
29. Wang T, et al. TGF-beta-induced miR-21 negatively regulates the antiproliferative activity but has no effect on EMT of TGF-beta in HaCaT cells. *Int J Biochem Cell Biol*. 2012; 44:366–376. [PubMed: 22119803]
30. Zhong X, Chung AC, Chen HY, Meng XM, Lan HY. Smad3-mediated upregulation of miR-21 promotes renal fibrosis. *J Am Soc Nephrol*. 2011; 22:1668–1681. [PubMed: 21852586]
31. Yao Q, et al. Micro-RNA-21 regulates TGF-beta-induced myofibroblast differentiation by targeting PDCD4 in tumor-stroma interaction. *Int J Cancer*. 2011; 128:1783–1792. [PubMed: 20533548]
32. Kim YJ, Hwang SJ, Bae YC, Jung JS. MiR-21 regulates adipogenic differentiation through the modulation of TGF-beta signaling in mesenchymal stem cells derived from human adipose tissue. *Stem cells*. 2009; 27:3093–3102. [PubMed: 19816956]
33. Ma X, et al. Loss of the miR-21 allele elevates the expression of its target genes and reduces tumorigenesis. *Proceedings of the National Academy of Sciences of the United States of America*. 2011; 108:10144–10149. [PubMed: 21646541]
34. Zhu H, et al. MicroRNA Expression Abnormalities in Limited Cutaneous Scleroderma and Diffuse Cutaneous Scleroderma. *J Clin Immunol*. 2012; 32:514–522. [PubMed: 22307526]
35. Darido C, et al. Targeting of the tumor suppressor GRHL3 by a miR-21-dependent protooncogenic network results in PTEN loss and tumorigenesis. *Cancer cell*. 2011; 20:635–648. [PubMed: 22094257]
36. Narducci MG, et al. MicroRNA profiling reveals that miR-21, miR486 and miR-214 are upregulated and involved in cell survival in Sezary syndrome. *Cell Death Dis*. 2011; 2:e151. [PubMed: 21525938]
37. Oshimori N, Fuchs E. Paracrine TGF-beta signaling counterbalances BMP-mediated repression in hair follicle stem cell activation. *Cell stem cell*. 2012; 10:63–75. [PubMed: 22226356]
38. Sugawara K, Schneider MR, Dahlhoff M, Kloepper JE, Paus R. Cutaneous consequences of inhibiting EGF receptor signaling in vivo: normal hair follicle development, but retarded hair cycle induction and inhibition of adipocyte growth in *Egfr(Wa5)* mice. *Journal of dermatological science*. 2010; 57:155–161. [PubMed: 20060271]
39. Lowry WE, et al. Defining the impact of beta-catenin/Tcf transactivation on epithelial stem cells. *Genes & development*. 2005; 19:1596–1611. [PubMed: 15961525]
40. Kimura-Ueki M, et al. Hair Cycle Resting Phase Is Regulated by Cyclic Epithelial FGF18 Signaling. *The Journal of investigative dermatology*. 2012; 132:1338–1345. [PubMed: 22297635]
41. Kobiela K, Stokes N, de la Cruz J, Polak L, Fuchs E. Loss of a quiescent niche but not follicle stem cells in the absence of bone morphogenetic protein signaling. *Proceedings of the National Academy of Sciences of the United States of America*. 2007; 104:10063–10068. [PubMed: 17553962]
42. Brownstein MH, Mehregan AH, Bilowski JB. Trichilemmomas in Cowden's disease. *Jama*. 1977; 238:26. [PubMed: 577252]
43. Lazarov M, et al. CDK4 coexpression with Ras generates malignant human epidermal tumorigenesis. *Nature medicine*. 2002; 8:1105–1114.

44. Agrawal N, et al. Exome sequencing of head and neck squamous cell carcinoma reveals inactivating mutations in NOTCH1. *Science (New York, N.Y.)*. 2011; 333:1154–1157.
45. Stransky N, et al. The mutational landscape of head and neck squamous cell carcinoma. *Science (New York, N.Y.)*. 2011; 333:1157–1160.
46. Kubo Y, Urano Y, Hida Y, Arase S. Lack of somatic mutation in the PTEN gene in squamous cell carcinomas of human skin. *Journal of dermatological science*. 1999; 19:199–201. [PubMed: 10215192]
47. Al-Zaid T, et al. Trichilemmomas show loss of PTEN in Cowden syndrome but only rarely in sporadic tumors. *Journal of cutaneous pathology*. 2012; 39:493–499. [PubMed: 22486434]
48. Kurose K, Zhou XP, Araki T, Eng C. Biallelic inactivating mutations and an occult germline mutation of PTEN in primary cervical carcinomas. *Genes, chromosomes & cancer*. 2000; 29:166–172. [PubMed: 10959096]

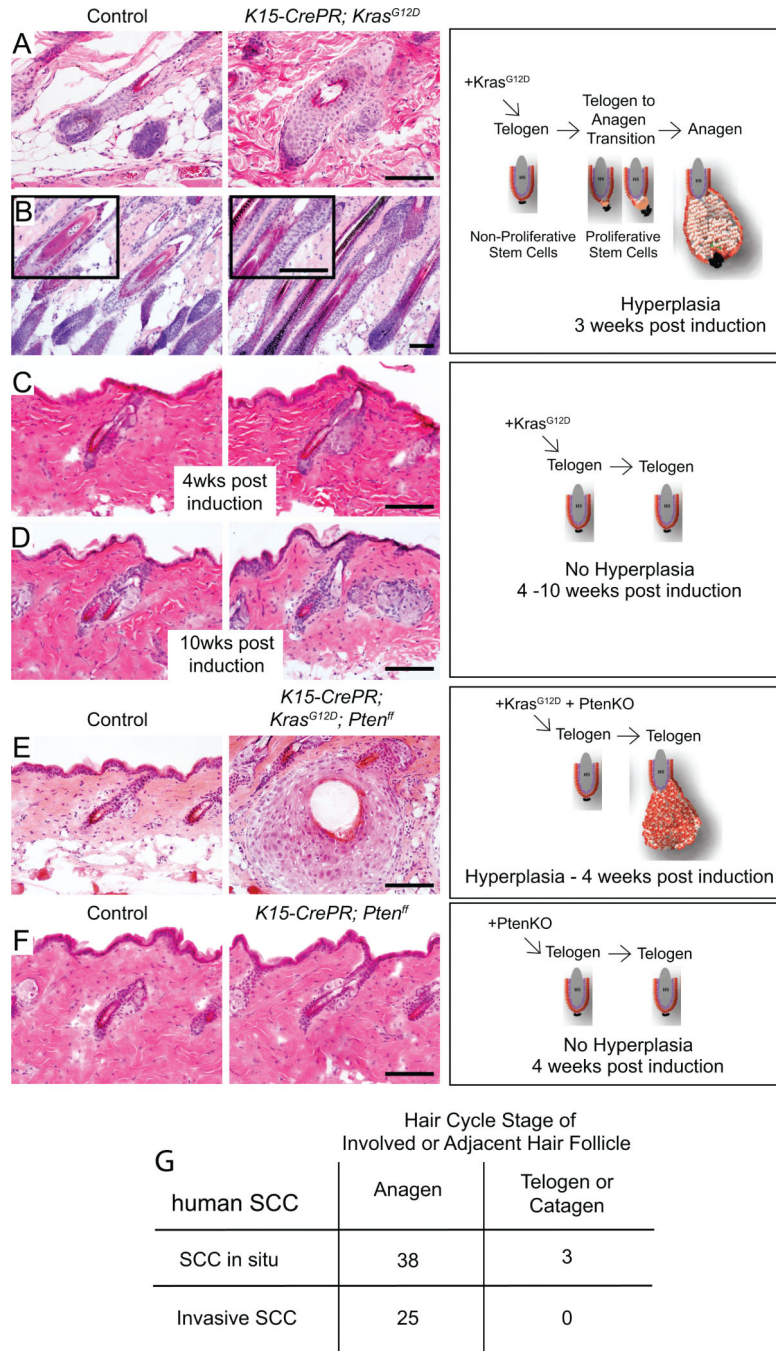


**Figure 1. Pten mediates stem cell quiescence based tumor suppression**

A, B) Hair follicle stem cells targeted to express *Kras<sup>G12D</sup>* demonstrate hyperplasia immediately following a telogen to anagen transition (A) and hyperplasia of the outer root sheath within 3 weeks post mifepristone administration (B). C and D) By contrast, hair follicle stem cells targeted to express oncogenic *Kras* during hair follicle stem cell quiescence are comparable to controls, demonstrating no hyperplastic expansion at either four weeks (C) or ten weeks (D) post induction by mifepristone. E) *Pten* deletion alleviates quiescence based tumor suppression and facilitates *Kras<sup>G12D</sup>* mediated bulge hyperplastic

expansion within four weeks. F) *Pten*-only deletion during hair follicle stem cell quiescence does not result in hyperplasia or initiation of anagen via stem cell activation. G) Examination of human SCC shows that most tumors are associated with anagen follicles. Panel A, C-F and Panel B insets shown at 20X. Panel B shown at 10X. Scale bar represents 100 $\mu$ M.

Author Manuscript

Author Manuscript

Author Manuscript

Author Manuscript

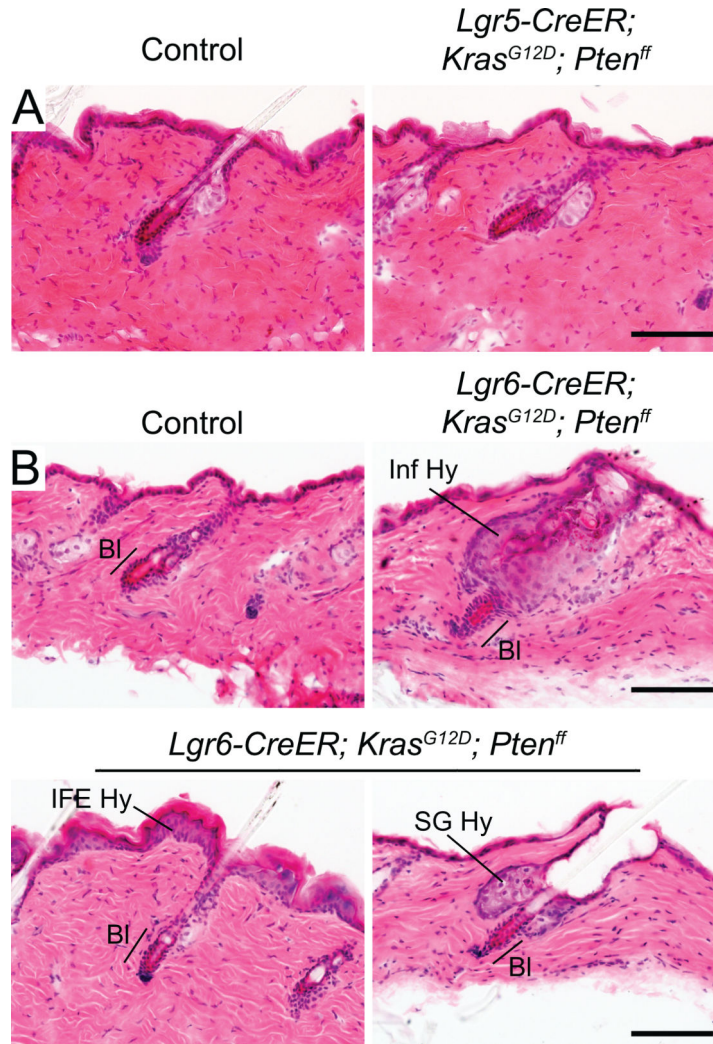


**Figure 2. *Lgr5* and *Lgr6* expressing cells of the telogen hair follicle do not respond to *Kras<sup>G12D</sup>* expression with *Pten* deletion**

A) Targeted expression of *Kras<sup>G12D</sup>* combined with *Pten* deletion to the hair germ and lower bulge does not initiate hyperplastic expansion over a four-week time course. Induced *Lgr5-CreER;Kras<sup>G12D</sup>;Pten<sup>ff</sup>* telogen bulges are comparable to controls. B) Expression of *Kras<sup>G12D</sup>* combined with *Pten* deletion to the *Lgr6*+ cells found above the bulge, and in some cells of the interfollicular epidermis, results in hyperplasias of the sebaceous gland, interfollicular epidermis and infundibular region. *Lgr6-CreER;Kras<sup>G12D</sup>;Pten<sup>ff</sup>* hyperplasias are morphologically distinct from the bulge hyperplasias found in *K15-CrePR;Kras<sup>G12D</sup>;Pten<sup>ff</sup>* telogen bulges (Figure 1E). SG Hy: sebaceous gland hyperplasia, IFE Hy: Interfollicular epidermis hyperplasia, Inf Hy: Infundibular region hyperplasia. All panels shown at 20X. Scale bar represents 100 $\mu$ M.

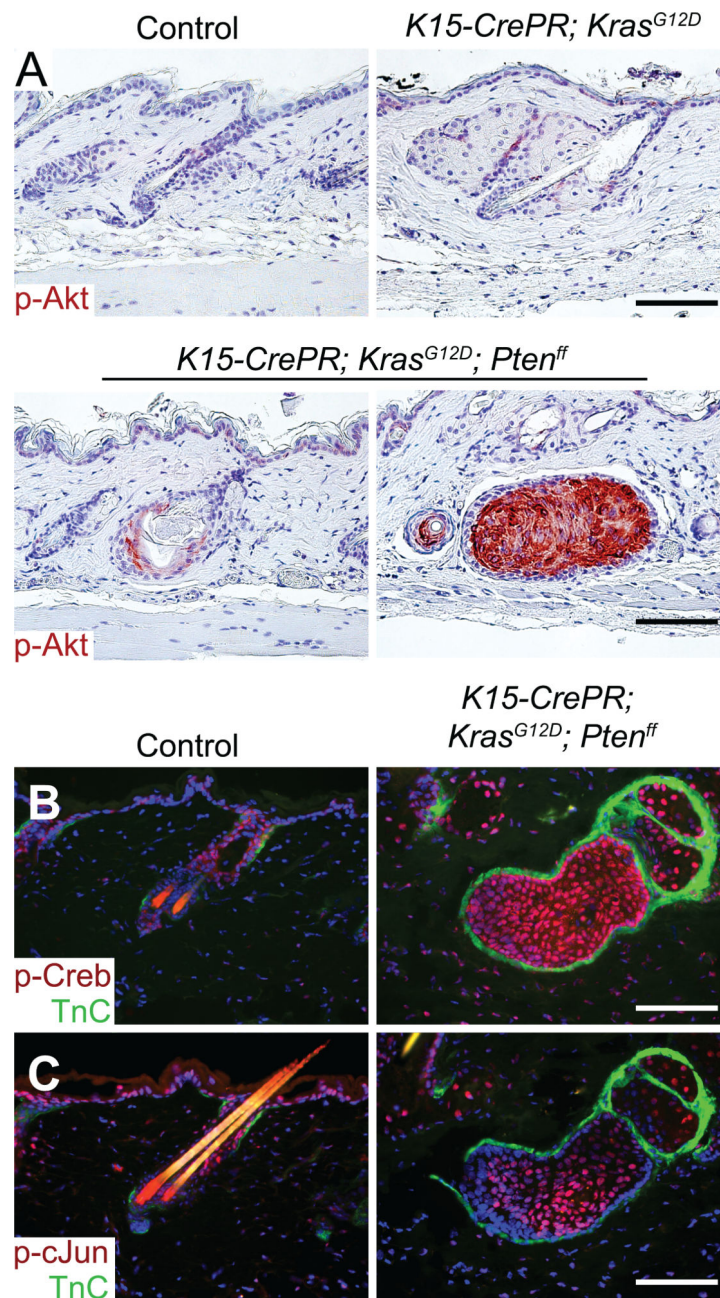


**Figure 3. Activity of signaling pathways and transcription factors downstream of Pten**  
 A) Phospho-Akt antibody staining shows no apparent activity in control and *Kras<sup>G12D</sup>* expressing telogen hair follicles (upper panels). Hyperplasias formed from telogen hair follicle stem cells exhibiting deletion of *Pten* combined with *Kras<sup>G12D</sup>* expression show high p-Akt staining, consistent with lack of Pten activity (lower panels). B) p-Creb stains at high levels and is localized to the nucleus in *K15-CrePR;Kras<sup>G12D</sup>;Pten<sup>ff</sup>* hyperplasias. Nuclear expression can be found in the infundibulum and hair germ of control tissue, but no apparent staining is found in the control bulge. C) Nuclear p-cJun, indicating JNK pathway activation, is found at high levels in *K15-CrePR;Kras<sup>G12D</sup>;Pten<sup>ff</sup>* bulge hyperplasias.

Control bulges do not show any apparent staining, but p-cJun is found in the interfollicular epidermis and infundibulum. All panels shown at 20X. Scale bar represents 100 $\mu$ M.

Author Manuscript

Author Manuscript

Author Manuscript

Author Manuscript



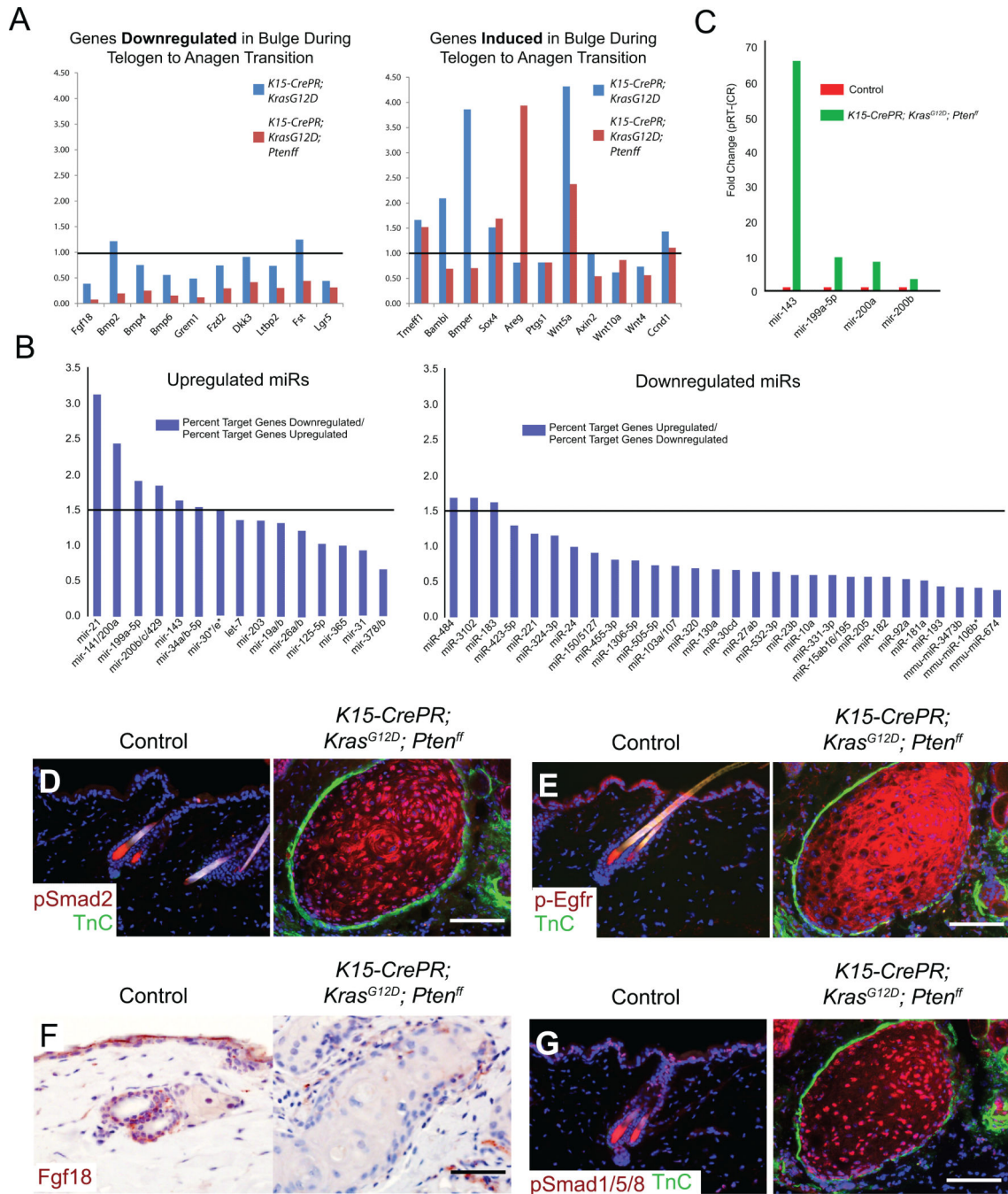


#### Figure 4. Defining mechanisms of action for Pten as a tumor suppressor in telogen

A) Following FACS isolation of *K15-CrePR;Kras<sup>G12D</sup>;Pten<sup>ff</sup>;LSLYFP<sup>+</sup>* cells, microarray profiling was performed. The panels in (A) show ratios of gene expression for the indicated genotype relative to control HFSCs for selected genes known to influence hair follicle stem cell activation and quiescence<sup>8,37</sup>. B) Histogram depicting ratio of percent target genes 2 fold or more downregulated divided by percent target genes 2 fold or more upregulated among miRNAs families upregulated 1.5 fold or more in YFP+ *K15-CrePR;Kras<sup>G12D</sup>;Pten<sup>ff</sup>;LSLYFP* cells compared to YFP+ *K15-CrePR;LSLYFP* cells. Target

genes of miR-21 were most commonly found amongst downregulated mRNAs, suggesting functional significance of miR-21 upregulation. B) lower, shows a histogram of ratio of mRNA target genes upregulated by two fold versus those downregulated in YFP+ *K15-CrePR;Kras<sup>G12D</sup>;Pten<sup>ff</sup>;LSLYFP* cells compared to YFP+ *K15-CrePR;LSLYFP* cells. This indicates that downregulation of just 3 miRNAs appeared to have a functional impact on mRNA levels. C) Histogram depicting selected miRNA changes in YFP+ *K15-CrePR;Kras<sup>G12D</sup>;Pten<sup>ff</sup>;LSLYFP* cells compared to YFP+ *K15-CrePR;LSLYFP* cells from an independent biological replicate by RT-PCR. D) Smad2, an obligate transducer of Tgf $\beta$  signals, is phosphorylated in hyperplasias but not in telogen controls. E) p-Egfr staining shows high levels of Egfr activity in *K15-CrePR;Kras<sup>G12D</sup>;Pten<sup>ff</sup>* hyperplasias compared to controls. F) Staining for Fgf18, known to maintain stem cell quiescence, was expressed in telogen control bulges but absent in *K15-CrePR;Kras<sup>G12D</sup>;Pten<sup>ff</sup>* hyperplasias. G) Bmp signaling, shown by phospho-Smad1/5/8, is high in *K15-CrePR;Kras<sup>G12D</sup>;Pten<sup>ff</sup>* hyperplasias and low in telogen controls. A-D shown at 20X. Scale bar represents 100 $\mu$ M.

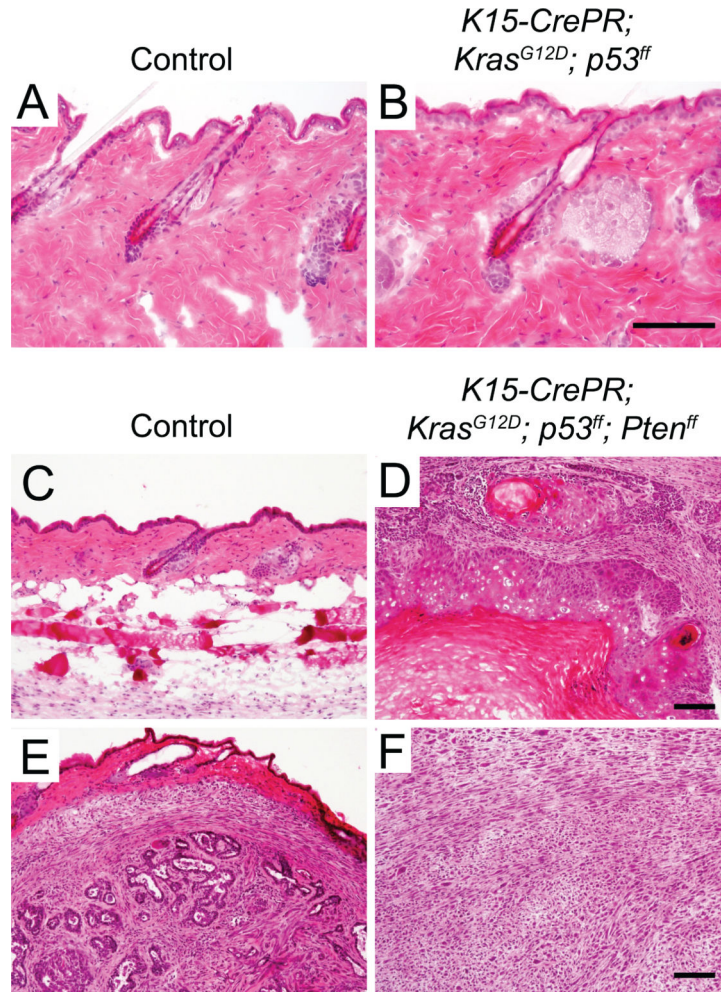


**Figure 5. Gain of *Kras*<sup>G12D</sup>, coupled with loss of both *Pten* and *p53* is sufficient to drive non-melanoma skin malignancies in otherwise quiescent HFSCs**  
 (A and B) Similar to *K15-CrePR;Kras*<sup>G12D</sup> hair follicles, *K15-CrePR;Kras*<sup>G12D</sup>;*p53*<sup>ff</sup> bulge cells are unable to initiate tumorigenesis during quiescence. (C – F) Additional deletion of *Pten*, however, facilitates formation of phenotypes that resemble several pathologically distinct skin malignancies, including malignant tricholemmoma (D), malignant trichoblastoma (E), and spindle cell squamous cell carcinoma (F). BI: bulge, SG: sebaceous gland, SG Hy: sebaceous gland hyperplasia. A, B shown at 20X. C – F shown at 10X. Scale bar represents 100 $\mu$ M.

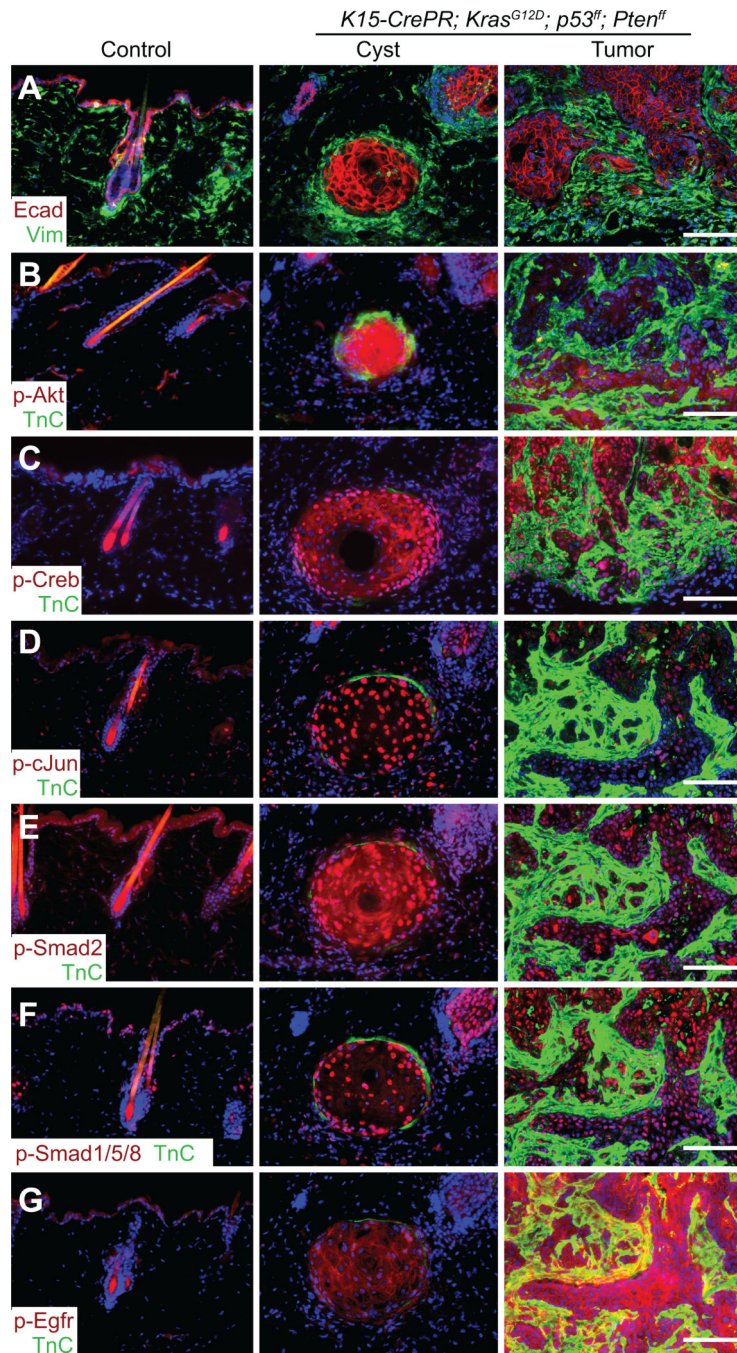


**Figure 6. Signaling pathways differentially regulated during progression of tumors in *K15-CrePR; Kras<sup>G12D</sup>; p53<sup>fl</sup>; Pten<sup>fl</sup>* skin**

The third column shows images from a large *K15-CrePR; Kras<sup>G12D</sup>; p53<sup>fl</sup>; Pten<sup>fl</sup>* driven SCC. Middle panel shows small cyst hyperplasia found nearby the mass depicted in the right panel. Hyperplasia (middle) in *K15-CrePR; Kras<sup>G12D</sup>; p53<sup>fl</sup>; Pten<sup>fl</sup>* demonstrates high E-cadherin (A), p-Akt (B), p-Creb (C), p-cJun (D), p-Smad2 (E), p-Smad1/5/8 (F), and p-Egfr (G), similar to *K15-CrePR; Kras<sup>G12D</sup>; Pten<sup>fl</sup>* skin. Tumors show high p-Creb (C), p-Smad2

(E), p-Smad1/5/8 (F) and p-Egfr (G), but low or absent p-Akt (B) and p-cJun (D). All panels shown at 20X. Scale bar represents 100 $\mu$ M.

Author Manuscript

Author Manuscript

Author Manuscript

Author Manuscript